Infectious Disease Modelling 9 (2024) 744–762

Contents lists available at ScienceDirect

Infectious Disease Modelling

journal homepage: www.keaipublishing.com/idm

Mathematical modeling for estimating influenza vaccine efficacy: A case study of the Valencian Community, Spain.

Carlos Andreu-Vilarroig [a], Rafael J. Villanueva [a], Gilberto González-Parra [a, b, *]

[a] Instituto de Matemática Multidisciplinar, Universitat Politècnica de València, Valencia, Spain
[b] Department of Mathematics, New Mexico Tech, Socorro, NM, USA

ARTICLE INFO

Article history:
Received 23 February 2024
Received in revised form 2 April 2024
Accepted 10 April 2024
Handling Editor: Dr Daihai He

Keywords:
Mathematical modeling
Epidemiology
SEIR
Vaccine efficacy
Influenza
Valencian community

ABSTRACT

Vaccine efficacy and its quantification is a crucial concept for the proper design of public health vaccination policies. In this work we proposed a mathematical model to estimate the efficacy of the influenza vaccine in a real-word scenario. In particular, our model is a SEIR-type epidemiological model, which distinguishes vaccinated and unvaccinated populations. Mathematically, its dynamics is governed by a nonlinear system of ordinary differential equations, where the non-linearity arises from the effective contacts between susceptible and infected individuals. Two key aspects of this study is that we use a vaccine distribution over time that is based on real data specific to the elderly people in the Valencian Community and the calibration process takes into account that over one influenza season a specific proportion of the population becomes infected with influenza. To consider the effectiveness of the vaccine, the model incorporates a parameter, the vaccine attenuation factor, which is related with the vaccine efficacy against the influenza virus. With this framework, in order to calibrate the model parameters and to obtain an influenza vaccine efficacy estimation, we considered the 2016–2017 influenza season in the Valencian Community, Spain, using the influenza reported cases of vaccinated and unvaccinated. In order to ensure the model identifiability, we choose to deterministically calibrate the parameters for different scenarios and we find the one with the minimum error in order to determine the vaccine efficacy. The calibration results suggest that the influenza vaccine developed for 2016–2017 influenza season has an efficacy of approximately 76.7%, and that the risk of becoming infected is five times higher for an unvaccinated individual in comparison with a vaccinated one. This estimation partially agrees with some previous studies related to the influenza vaccine. This study presents a new integrated mathematical approach to study the influenza vaccine efficacy and gives further insight into this important public health topic.

* Corresponding author.
E-mail addresses: caranvi1@upv.es (C. Andreu-Vilarroig), rjvillan@imm.upv.es (R.J. Villanueva), Gilberto.Gonzalezparra@nmt.edu (G. González-Parra).
Peer review under responsibility of KeAi Communications Co., Ltd.

https://doi.org/10.1016/j.idm.2024.04.006

1. Introduction

Every year, there are about a billion cases of seasonal influenza, with 3–5 million of those cases resulting in serious disease, and from 290,000 to 650,000 respiratory fatalities caused by the disease. In underdeveloped nations, lower respiratory tract infections caused by influenza account for 99% of mortality in children under the age of five. This impact is mainly due to the high transmissibility of the influenza virus. Droplets harboring viruses, known as infectious droplets, are released into the air when an infected person coughs or sneezes, and they can infect those nearby (World Health Organization (WHO), 2023). In congested locations like nursing homes and schools, seasonal influenza spreads even more quickly and easily. It has also been observed that seasonal epidemics primarily happen in the winter in temperate areas, although influenza can recur all year round in tropical places (Chadha et al., 2020; González-Parra, Villanueva, Ruiz-Baragaño, & Moraño, 2015; Hirve et al., 2016; Tamerius et al., 2011; Young & Chen, 2020; Yuan, Kramer, Lau, Cowling, & Yang, 2021). In order to decrease the number of people infected by influenza, the World Health Organization (WHO) strongly recommends the annual vaccination of the population. To date, is the most important resource to prevent influenza infections (World Health Organization (WHO), 2023). However, the vaccine coverage is not high in all group ages, especially in older age groups (European Centre for Disease Prevention and Control, 2018). This creates several public health problems, particularly for the elderly, as their mortality rate from infection and flu-like illnesses is higher compared to that of younger people (Clar, Oseni, Flowers, Keshtkar-Jahromi, & Rees, 2015; Warren-Gash, Smeeth, & Hayward, 2009). Some previous studies have investigated influenza vaccine hesitancy and its consequences (Dombrádi, Joó, Palla, Pollner, & Belicza, 2021; Fadl et al., 2023; Portero de la Cruz & Cebrino, 2020; Vila-Candel et al., 2016).

Vaccination programs offer direct and indirect defense against infectious diseases. On the one hand, direct protection reduces the likelihood that recipients of vaccinations may contract the disease or lessens the infectiousness of vaccinated individuals in the event of breakthrough infections. On the other hand, indirect protection reduces transmission within the community by lowering the rate of transmission for both vaccinated and unvaccinated individuals (Shim & Galvani, 2012). Unfortunately, a problematic aspect of the influenza virus is its high mutability, which causes new virus strains to emerge each season that coexist with previous ones. This fact makes it extremely difficult to find a vaccine valid for all seasons, and requires that it must be changed every year. For this reason, each year, the WHO makes recommendations on the makeup of influenza virus vaccines for the upcoming season based on an analysis of the circulating strains in the initial places where outbreaks occur (World Health Organization (WHO), 2023). In particular, the WHO recommends vaccine updates in February for the Northern Hemisphere and September for the Southern Hemisphere (Paules, Sullivan, Subbarao, & Fauci, 2018). Unfortunately, the random nature of the virus reassortment makes the spread of the virus and the appearance of other strains uncertain. It has been mentioned in several studies that a universal seasonal vaccine that provides a broad cross-immunity reduces the likelihood of pandemic emergence (Zhang et al., 2014). Moreover, the antigenic distance between the seasonal circulating strains and the vaccine strains affects the vaccine efficacy (Morimoto & Takeishi, 2018). Thus, when the antigens in an influenza vaccination are similar to those of circulating strains, the vaccine is more effective (Jefferson, Rivetti, Harnden, Di Pietrantonj, & Demicheli, 2008; Morimoto & Takeishi, 2018; Paules et al., 2018; Tricco et al., 2013). There are always various closely related influenza strains circulating and vaccines are designed taking into account antigenic and genetic characterization and forecasting which strains would circulate in the next season (Paules et al., 2018). Calculating the vaccine efficacy after the influenza season ends (which typically occurs in April or May in the northern hemisphere) is highly recommended in order to improve the vaccine development process, even though effectiveness can be studied (and measured) from different points of view, and oftentimes there is a lack of reliable data.

In (Lopez & Legge, 2020) a review that focuses on the immune basis of influenza vaccines is presented. The authors mentioned the cross-protection of influenza vaccines against heterologous influenza viruses and also the immunity provided by natural influenza virus infection. In (Tricco et al., 2013) a systematic review and meta-analysis of the influenza vaccines efficacy is presented. It includes the analysis of data on 47 influenza seasons and it was found that influenza vaccines provide protection against non-matching circulating strains (Johansen et al., 2024). The confidence intervals for the vaccine efficacy for children provided a minimum value of 28% and a maximum value of 90% for mismatched circulated strains. For the matched ones, the minimum value was 54% and, the maximum value, 88%. This is a high variability due to several factors such as the seasonal variations of the influenza strains and the type of virus. The annual influenza vaccine efficacy fluctuates and it has been estimated to be in the 30–60% range, against influenza-like illness (Gupta, Earl, & Deem, 2006). In (Quach, Mallis, & Cordero, 2020) the authors mentioned that the seasonal vaccine was protective against laboratory-confirmed influenza, but not protective against influenza-like illness or respiratory illness. This shows the difficulty and issues of the vaccine efficacy and effectiveness concepts.

In the USA and Europe, different reports have been published with the aim of studying the estimation of the influenza vaccine effectiveness (Centers for Disease Control and Prevention (CDC), 2023; Diaz-Granados, Denis, & Plotkin, 2012; Gjini & Gomes, 2016; Kissling & Rondy, 2017). There are different definitions of vaccine efficacy and effectiveness (Basta, Halloran, Matrajt, & Longini, 2008; Gjini & Gomes, 2016; Gupta et al., 2006; Quach et al., 2020; Shim & Galvani, 2012). The ability of vaccinations to prevent influenza and its complications in the best of situations, like in a clinical trial, is known as efficacy. On the other hand, the ability of a vaccine to fend off influenza and its associated complications in everyday circumstances of medical practice, including observational studies, is known as its effectiveness (Quach et al., 2020). It has been mentioned that the vaccine efficacy is in the 40–90% range (Diaz-Granados et al., 2012). In (Gjini & Gomes, 2016), the authors define vaccine efficacy as the reduction of the probability of pathogen acquisition per contact. Other methods compare attack rates in

vaccinated and unvaccinated individuals, or use the vaccination status of the infected individuals relative to the population vaccination coverage. In (Diaz-Granados et al., 2012) a systematic review with meta-analyses of controlled trials was performed and it was found that the vaccine efficacy was 65% against any strain.

In (Shim & Galvani, 2012) it has been argued that the definition of vaccine efficacy and effectiveness must be stated explicitly in order to avoid the incorrect parameterization of epidemiological models. In (Shim & Galvani, 2012) the authors stated that the vaccine efficacy quantifies the difference between a vaccinated person risk of infection and that of an unvaccinated person in order to determine the protective effects of vaccination. In contrast, vaccine effectiveness is different and can be classified as direct, indirect, total and overall (Haber, Longini, & Halloran, 1991; Halloran, Struchiner, & Longini, 1997).

In all this context, there is little study of vaccine efficacy from a mathematical modeling perspective. Few papers have studied the impact of vaccine efficacy by using dynamic epidemiological models that are based on differential equations (Gjini & Gomes, 2016; Martínez-Rodríguez, Navarro-Quiles, San-Julián-Garcés, & Villanueva, 2020; Yin, Lu, Du, & Shi, 2022). In (Martínez-Rodríguez et al., 2020), the authors used an epidemiological model to estimate the vaccine efficacy by fitting the model to prevalence data post-vaccination. In (Gjini & Gomes, 2016) the authors used SI and SIS epidemiological models to show how the relationship between prevalence ratios in vaccinated and non-vaccinated hosts depend on true vaccine efficacy and infection rate of the pathogen. There are other works that have used mathematical models to observe the effects of the vaccine efficacy for influenza and recently for COVID-19 pandemic (Demongeot, Griette, Magal, & Webb, 2022; Hughes et al., 2020; Mahmud et al., 2022; Martínez-Rodríguez, Gonzalez-Parra, & Villanueva, 2021; Mercer, Barry, & Kelly, 2011; Ratti et al., 2022; Van Effelterre, Dos Santos, & Shinde, 2016).

The aim of this paper is to present a mathematical model to describe the transmission dynamics of the influenza and whose structure allows us to identify the vaccine efficacy in a real-world scenario. Estimating the vaccine efficacy using real data and a mathematical model is challenging since there are several factors that affect the dynamics of influenza and the underlying assumptions of the mathematical models. The constructed model is based on the Susceptible-Exposed-Infected-Recovered (SEIR) framework that considers the cross-immunity of individuals due to previous exposure to different influenza strains and vaccination from previous seasons. The model dynamics is governed by a nonlinear system of differential equations, where the unvaccinated and vaccinated populations are distinguished and modeled separately. The non-linearity comes from the effective contacts between susceptible and infected individuals, which is the main driving force of the influenza virus spread. A crucial aspect of this study is that we use a vaccine distribution over the time that is based on real data specific to the Valencian Community. To the best of our knowledge this has not been implemented in previous studies. This aspect is important in order to have a more realistic analysis and to assess the vaccine efficacy. The specific vaccine distribution could vary over different countries depending on people's behavior and the public health system. For instance, in (Van Effelterre et al., 2016) it was found by mathematical modeling that in Norway during the 2009 pandemic more than 50% of the vaccinated people may already have been infected before being vaccinated. This aspect could change if the vaccination program starts early before the peak of the influenza season.

In order to quantify the vaccine efficacy, the model includes an embedded parameter, the so-called vaccine attenuation factor, which is related with the vaccine efficacy against the influenza virus. With regard to measuring vaccine efficacy we rely on a simple definition: we measure the vaccine efficacy by the difference between a vaccinated person's risk of infection and that of an unvaccinated person (Haber et al., 1991; Shim & Galvani, 2012). There are other approaches to measure vaccine efficacy under different contexts. In the real-world case, the vaccine efficacy is obtained by a calibration process, which finds the unknown parameters of the model (including the vaccine attenuation factor) that best fit the real data. In our case, we use the reported influenza cases from the Valencian Community in the 2016–2017 season for calibration. In order to ensure the model identifiability, some important restrictions were added to the model. One key information that is used in the calibration process is that it has been estimated that the number of people who end up getting the seasonal flu each year is between 5 and 15% (Departamento de Seguridad Nacional, 2023; Russell et al., 2008; Stöhr, 2002; Tokars, Olsen, & Reed, 2018). Thus, in order to satisfy this constraint we can obtain a range of values for the influenza transmission rate which reduces the search space and helps with the identifiability of the parameters of the model. Another key information that is used in the calibration process is that there is a time-varying distribution of reported cases in vaccinated and unvaccinated cases. This distribution is estimated by using real data and taking into account the percentage of vaccinated people over time. Finally, the calibration process considers a standard rescaling on the infected data curve of the model in order to fit it with the reported cases.

The paper is organized as follows. In Section 2, we describe the proposed mathematical model (Section 2.1), the vaccine efficacy quantification (Section 2.2), the data (Section 2.3) and the model parameters in detail (Section 2.4). Then, the complete calibration process, with the minimization problem (Section 2.5) and the posterior error function analysis (Section 2.6) are also explained. The calibration results obtained from the calibration process are presented and discussed in Section 3. Finally, some relevant conclusions are given in Section 4.

2. Materials and methods

In this section, we first describe the epidemiological mathematical model that attempts to describe the dynamics of seasonal influenza. The selected model is of the compartmental type, i.e., it subdivides the total population into several subpopulations of interest. The variation of these populations over time is governed by a system of first-order differential equations, which are characterized by a set of parameters, some of which are unknown. The model calibration process aims to

find these unknown model parameters that best fit a set of real data. In this case, a deterministic calibration has been proposed, i.e., the parameter values are considered deterministic (exact) values. For the model and calibration process application, the influenza season of 2016–2017 in the Valencian Community has been taken as the case study scenario. The reported case data consist of weekly reported influenza cases.

2.1. Model description

The compartmental epidemiological model divides the population into the following subpopulations (compartments) for each time $t \geq 0$:

- $S_u(t)$: unvaccinated susceptible, i.e., those unvaccinated people who have not passed the infection and can be infected at time instant t.
- $S_v(t)$: vaccinated susceptible, i.e., those vaccinated people who have not passed the infection and can be infected at time instant t.
- $L_u(t)$: unvaccinated latent people, i.e., those unvaccinated people who have been infected but cannot infect the others at time instant t.
- $L_v(t)$: vaccinated latent people, i.e., those vaccinated people who have been infected but cannot infect the others at time instant t.
- $I_u(t)$: unvaccinated infected people, i.e., those unvaccinated people who have been infected and can infect the others at time instant t.
- $I_v(t)$: vaccinated infected people, i.e., those vaccinated people who have been infected and can infect the others at time instant t.
- $R_u(t)$: unvaccinated recovered people, i.e., those unvaccinated people who have passed the infection at time instant t.
- $R_v(t)$: unvaccinated recovered people, i.e., those vaccinated people who have passed the infection at time instant t.

In this model, which is focused on modeling a single influenza season, it will be assumed that the total population

$$N = N(t) = S_u(t) + S_v(t) + L_u(t) + L_v(t) + I_u(t) + I_v(t) + R_u(t) + R_v(t)$$

is constant. This assumption is plausible for populations in which births, deaths and migratory movements occur at very low rates and generate insignificant variations with respect to the total population (Hethcote, 1994).

The natural process of infection due to influenza virus, shown in Fig. 1, is the following:

1. A susceptible individual becomes latent by contact with other infected individuals. Thus, the susceptible population decreases proportionally to the number of contacts between susceptibles and infecteds. This is modeled with the $S(t)I(t)$ product term, with a proportionality constant $\frac{\beta}{N}$, which is related to the contact rate and the probability that a contact results in an infection. In the vaccinated population, the infection rate β is attenuated by a factor a_v due to the partial immunity conferred by the vaccine. It is important to remark that the attenuation factor a_v can be interpreted as a measure of vaccine efficacy because the expression $1 - a_v$ represents the reduction of the probability of influenza acquisition per contact caused by the vaccine (Gjini & Gomes, 2016).
2. A latent individual becomes infected after a latency period $\frac{1}{\lambda}$ days. It is known that, after infection, symptoms appear in an incubation or latency period of 2 days, although it can vary between 1 and 4 days (Centers for Disease Control and Prevention (CDC), 2023). In this study, we assume a value of $\lambda = 1/2$ days$^{-1} = 7/2$ weeks^{-1}.
3. An infected individual becomes recovered after an infectious period $\frac{1}{\gamma}$ days. In this period, the individual can infect other susceptible people. It is estimated that the infection time of an individual is between 5 and 7 days, although in certain individuals it may be longer (Centers for Disease Control and Prevention (CDC), 2023). In this study, we assume a value of $\gamma = 1/7$ days$^{-1} = 1$ weeks^{-1}.

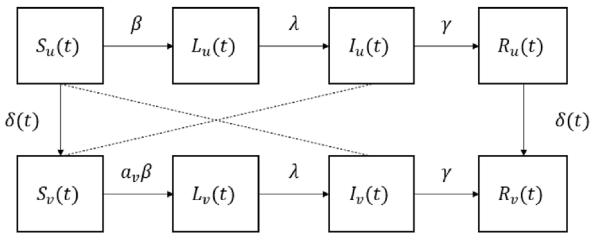

Fig. 1. Diagram of model (1). The unvaccinated and vaccinated populations are related through the contacts between susceptible and infected.

It is also assumed that recovered individuals cannot reinfect due to the natural immunity that do not wane over one influenza season. Additionally, during the season there is a part of the population that is progressively vaccinated.

The dynamics of the model is governed by the following system of differential equations:

$$\begin{aligned}
\dot{S}_u(t) &= -\beta \frac{S_u(t)[I_u(t)+I_v(t)]}{N} - \delta(t) S_u(t), \\
\dot{S}_v(t) &= -a_v \beta \frac{S_v(t)[I_u(t)+I_v(t)]}{N} + \delta(t) S_u(t), \\
\dot{L}_u(t) &= \beta \frac{S_u(t)[I_u(t)+I_v(t)]}{N} - \lambda L_u(t), \\
\dot{L}_v(t) &= a_v \beta \frac{S_u(t)[I_u(t)+I_v(t)]}{N} - \lambda L_v(t), \\
\dot{I}_u(t) &= \lambda L_u(t) - \gamma I_u(t), \\
\dot{I}_v(t) &= \lambda L_v(t) - \gamma I_v(t), \\
\dot{R}_u(t) &= \gamma I_u(t) - \delta(t) R_u(t), \\
\dot{R}_v(t) &= \gamma I_v(t) + \delta(t) R_u(t),
\end{aligned} \tag{1}$$

where $\beta \in \mathbb{R}_+$ is the infection rate, $a_v \in [0,1]$ is the vaccine attenuation factor, $1/\lambda \in \mathbb{R}_+$ is the average incubation time, $\gamma \in \mathbb{R}_+$ is the recovery rate and $\delta(t) \in \mathbb{R}_+$ is the vaccination rate. Notice that susceptible individuals acquire the influenza virus at a rate $f(t)$, which is the force of infection and is given by

$$f(t) = \beta \frac{I_u(t)+I_v(t)}{N} + a_v \beta \frac{I_u(t)+I_v(t)}{N} \tag{2}$$

The parameters of model (1), with their description, known values and units, are summarized in Table 1.

It should be noted that in this study we assume that the vaccinated and unvaccinated people have the same latency λ and recovery γ rates on average. This means that vaccinated and unvaccinated individuals spend the same latency/exposed period (from the time the virus enters them until they can infect others) and the same recovery time (they spend the same number of days being infectious). Although in reality there could be differences between vaccinated and unvaccinated, we assume that these differences in days are not significant in a disease whose dynamic evolution lasts for months. In (Romagosa et al., 2011) it was found that there is no significant difference with regard to the infectious period in vaccinated and unvaccinated pigs. In addition, in (van der Goot, van Boven, Koch, & de Jong, 2007), the difference of the infectious period between vaccinated and unvaccinated pheasants was less than 10%. However, it has been found that in chickens there is difference in the variability of the variance of the latent and infectious periods (Poetri et al., 2011). Regarding the latency period, it has been found in different works that it varies from a few hours to four days (Jing, Huo, & Xiang, 2020; Macdonald & Lyth, 1918; Centers for Disease Control and Prevention (CDC), 2023).

In the absence of a vaccine and without vital dynamics the SEIR model has a basic reproduction number given by $\mathcal{R}_0 = \beta/\gamma$. For the SEIR model, if vital dynamics and constant population are considered then $\mathcal{R}_0 = \beta\lambda/[(\lambda+\mu)(\gamma+\mu)]$, where μ represents both the birth and death rates (Hethcote, 2000). Note, that oftentimes the vital dynamics are much slower that the disease progression. Then, even for the SEIR model one gets that $\mathcal{R}_0 \approx \beta/\gamma$. In this study we focus on only one influenza season which can be considered very short dynamics. Therefore, the latency period and the basic reproduction number $\mathcal{R}_0$ become less relevant (Hethcote & van den Driessche, 1991). Although, one relevant threshold for one influenza season dynamics is the effective reproduction number $\mathcal{R}_e(t) = S(0)\mathcal{R}_0/N(t)$. If $\mathcal{R}_e(t) > 1$, the infected cases increase, if $\mathcal{R}_e(t) = 1$, the cases reach a peak and if $\mathcal{R}_e(t) < 1$, the cases decrease (Gumel, Iboi, Ngonghala, & Elbasha, 2021; Nishiura & Chowell, 2009). Notice that in this study the initial number of susceptible is given by $S(0) = S_u(0) + S_v(0)$. Then if $S(0)$ is significantly smaller than the whole population $N(t)$, then, one gets that $\mathcal{R}_e(t) \ll \mathcal{R}_0$ and a relatively large infection rate β is needed in order that the number of infected cases (both vaccinated and unvaccinated) increases. We will see that for the calibration process that includes a

Table 1
Model (1) parameters, with their description, known values and units.

Parameter	Description	Units	Value
β	Infection rate	time units^{-1}	For calibration
a_v	Vaccine attenuation factor	adimensional	For calibration
λ	Latency rate	time units^{-1}	1/2 days^{-1} (Centers for Disease Control and Prevention (CDC), 2023)
γ	Recovery rate	time units^{-1}	1/7 days^{-1} (Centers for Disease Control and Prevention (CDC), 2023)
$\delta(t)$	Vaccination rate	time units^{-1}	Real data (Portero et al., 2017)

variety of scenarios regarding $R(0)$, and therefore for $S(0)$, this previous aspect plays a crucial role in determining the vaccine efficacy.

2.2. Estimation of the vaccine efficacy

There are many available methodologies to compute the efficacy and the effectiveness of a vaccine. In fact, some works use these two definitions in an interchangeable way. However, the efficacy and effectiveness of a vaccine represent different concepts. In (Shim & Galvani, 2012), it has been argued that the definition of vaccine efficacy and effectiveness must be stated explicitly in order to avoid the incorrect parameterization of epidemiological models.

Let us briefly introduce these concepts and then define how we will measure the efficacy of the vaccine in this study. In (Quach et al., 2020), they define the effectiveness as the ability of a vaccine to fend off influenza and its associated complications in everyday circumstances of medical practice. In (Tentori, Passerini, Timberlake, & Pighin, 2021) mentioned that the vaccine efficacy can be calculated by using a double-blind, randomized, controlled trial where 50% of the subjects are vaccinated and the others just receive a placebo. Thus, they computed the vaccine efficacy (VE) as

$$\mathrm{VE} = \frac{\mathrm{ARU} - \mathrm{ARV}}{\mathrm{ARU}} \times 100 = (1 - \mathrm{RR}) \times 100, \tag{3}$$

where ARU and ARV are the attack rates among unvaccinated and vaccinated groups, respectively (Weinberg & Szilagyi, 2010). The term RR refers to relative risk of suffering the disease for vaccinated compared to unvaccinated subjects. This definition has the inconvenience of performing a double-blind randomized, controlled trial. In (Gjini & Gomes, 2016), the authors define vaccine efficacy as the reduction of the probability of pathogen acquisition per contact. Notice that this definition varies from the previous ones.

In (Haber et al., 1991; Shim & Galvani, 2012) the authors stated that the vaccine efficacy quantifies the difference between a vaccinated person risk of infection and that of an unvaccinated person in order to determine the protective effects of vaccination. In this study we measure the vaccine efficacy by the difference between a vaccinated person risk of infection and that of an unvaccinated person (Haber et al., 1991; Shim & Galvani, 2012). Thus, we use the model parameter a_v to measure the vaccine efficacy (VE) as

$$\mathrm{VE} = (1 - a_v) \times 100. \tag{4}$$

2.3. Data

In this subsection we present the data that is used for the calibration of the model (1). The available data for the calibration process are the following:

- The population size of the Valencian Community was $N = 4\,959\,968$ at the end of 2016 (Instituto Nacional de Estadística (INE), 2023). It can be seen that the annual population variations between years 2015–2016 and 2017–2018 were around -0.42% and -0.37%, respectively. Thus, it is reasonable to assume a constant population during the months of flu season.
- The weekly influenza reported incidence (cases/100 000 inhabitants) in the Valencian Community during the 2016–2017 season, with $n = 36$ weeks (37 weeks in total) (Portero et al., 2017). To obtain the reported influenza cases $\{I_r^{t_i}\}_{i=0}^{n}$, the incidence data were multiplied by N and divided by 100 000 (see Fig. 2a and Table 2). In order to fix the initial infected condition $I(0)$, we extended the data series by adding the previous 4 weeks (1 month) before the first week in which they were reported to have reported. In these weeks there were no reported cases, but influenza was already present in the population.

As it can be observed, the peak of reported infected cases is around week 20 (week 16 since cases start to be reported), which is similar to what have been obtained in previous works. For instance, for the seasonal influenza season of 2016–2017 in Puerto Rico (USA) it was found to peak around week 14 (Magal & Webb, 2018). Even though the Valencian Community and Puerto Rico have similarities their population structure and social behavior is different.

- Vaccination coverage in the Valencian Community during the 2015–2016 season was $c_v = 0.1423$ (14.23%). It has been computed knowing that 708 999 individuals were vaccinated over a total of 4 980 689 individuals that make up the Valencian Community population during the 2015–2016 season (Valenciana, 2023). The proportion of reported vaccinated cases at the end of the 2015–2016 season was $p_{rv} = 0.0453$ (4.53%) (Valenciana, 2023). The use of data from the 2015–2016 season is due to the lack of data from the 2016–2017 season of interest, assuming that these are similar between seasons. Finally, the vaccination distribution $\{\delta^{t_i}\}_{i=0}^{n}$ for the elderly population (>60 years-old) over the season 2016–2017 adjusted for the vaccination coverage was as shown in Table 2 and Fig. 2b (Portero et al., 2017). Although we

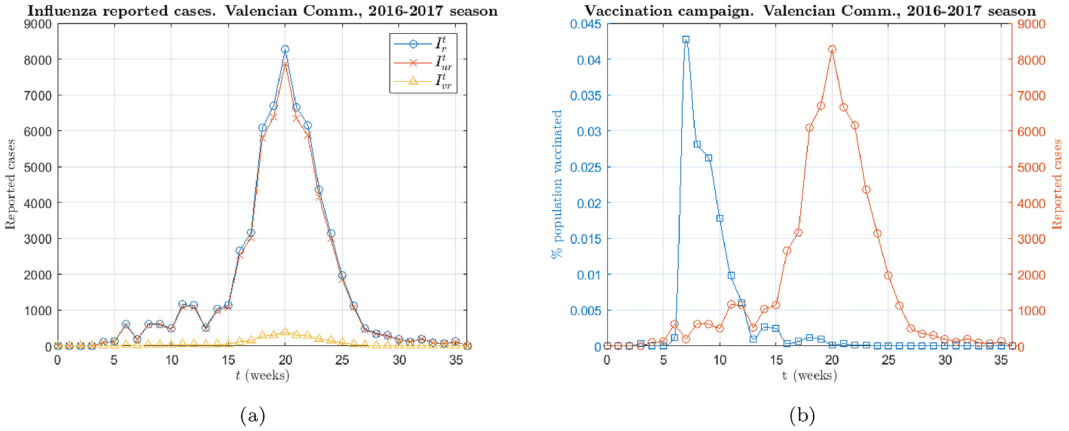

Fig. 2. Available data series for the 2016–2017 influenza season in the Valencian Community: (a) total, vaccinated and unvaccinated infected reported cases, and (b) vaccination percentage (over total population) vs. total infected reported cases (Portero et al., 2017).

did not have vaccination data for the entire population, but only for the elderly, we know that a large part of the vaccination campaign is focused on this group. Then, we have assumed that the total vaccination coverage curve over the time is not significantly different from the elderly one. Consequently, we assumed that the available vaccination real data distribution, adjusted for vaccination coverage, could be used for the total population.

Table 2
Data set collected for model calibration (Portero et al., 2017).

Week t	Incidence $\left(\frac{\textbf{cases}}{100000\text{inhab.}}\right)$	Reported cases I_r^t	Unvacc. reported cases I_{ur}^t	Vacc. reported cases I_{vr}^t	Vacc. rate δ^t (%N)
0	0.00	0.00	0.00	0.00	0.00
1	0.00	0.00	0.00	0.00	0.00
2	0.00	0.00	0.00	0.00	0.00
3	0.00	0.00	0.00	0.00	0.03
4	2.17	107.63	102.57	5.06	0.00
5	2.72	134.91	128.57	6.35	0.00
6	12.36	613.05	584.22	28.83	0.12
7	3.94	195.42	186.23	9.19	4.27
8	12.64	626.94	597.45	29.49	2.81
9	12.50	619.99	590.84	29.16	2.63
10	9.92	492.03	468.89	23.14	1.78
11	23.51	1166.08	1111.24	54.85	0.98
12	22.96	1138.81	1085.25	53.56	0.60
13	10.33	512.36	488.27	24.10	0.10
14	20.92	1037.63	988.82	48.80	0.27
15	23.10	1145.75	1091.86	53.89	0.25
16	53.53	2655.07	2530.19	124.88	0.03
17	63.86	3167.44	3018.46	148.98	0.07
18	122.69	6085.38	5799.17	286.22	0.12
19	135.19	6705.38	6390.00	315.38	0.10
20	166.71	8268.76	7879.85	388.91	0.02
21	134.10	6651.32	6338.48	312.83	0.03
22	124.18	6159.29	5869.60	289.69	0.02
23	87.77	4353.36	4148.61	204.75	0.02
24	63.45	3147.10	2999.08	148.02	0.00
25	39.54	1961.17	1868.93	92.24	0.00
26	22.83	1132.36	1079.10	53.26	0.00
27	9.78	485.08	462.27	22.82	0.00
28	7.20	357.12	340.32	16.80	0.00
29	5.98	296.61	282.66	13.95	0.00
30	3.94	195.42	186.23	9.19	0.00
31	2.45	121.52	115.80	5.72	0.00
32	4.21	208.81	198.99	9.82	0.00
33	2.04	101.18	96.42	4.76	0.00
34	1.36	67.46	64.28	3.17	0.00
35	2.58	127.97	121.95	6.02	0.00
36	0.41	20.34	19.38	0.96	0.00

Given this vaccination information, the series of reported cases was separated into the series of vaccinated $\{I_{rv}^{t_i}\}_{i=0}^{n}$ and unvaccinated $\{I_{ru}^{t_i}\}_{i=0}^{n}$ reported cases. For this purpose, it was considered that at each time t_i, there is a proportion of reported vaccinated cases $v^{t_i} = \hat{p}_{rv}\Delta^{t_i}$, so that

$$\begin{aligned} I_{rv}^{t_i} &= v^{t_i} I_r^{t_i} = (\hat{p}_{rv}\Delta^{t_i}) I_r^{t_i}, \\ I_{ru}^{t_i} &= (1 - v^{t_i}) I_r^{t_i} = (1 - \hat{p}_{rv}\Delta^{t_i}) I_r^{t_i}. \end{aligned}$$

Note that proportion of reported vaccinated v^{t_i} is proportional to the accumulated percentage of vaccinated (i.e., the vaccination rate) $\Delta^{t_i} = \sum_{j=1}^{t_i} \delta^j$, with a proportionality factor $\hat{p}_{rv}$. As, at the end of season, the proportion of must be equal to the proportion of unvaccinated $p_{rv} = 0.0453$, the proportionality factor $\hat{p}_{rv}$ can be estimated as

$$\frac{\sum_{i=1}^{n} I_{rv}^{t_i}}{\sum_{i=1}^{n} I_r^{t_i}} = \sum_{i=1}^{n} \frac{\hat{p}_{rv}\Delta^{t_i} I_r^{t_i}}{\sum_{i=1}^{n} I_r^{t_i}} = p_{rv} = 0.0453,$$

so that

$$\hat{p}_{rv} = \frac{\sum_{i=1}^{n} I_r^{t_i}}{\sum_{i=1}^{n} \Delta^{t_i} I_r^{t_i}} p_{rv} = 0.0470 \ (4.73\%).$$

Notice that the separation of the reported in vaccinated and unvaccinated cases enables to enrich the available data and improve the identifiability of the parameters of the model (Cole, 2020; Kreutz, Raue, & Timmer, 2012; Magal & Webb, 2018; Raue, Kreutz, Theis, & Timmer, 2013).

- It has been estimated that the number of people who end up getting the seasonal flu each year is between 5 and 15% (Departamento de Seguridad Nacional, 2023; Russell et al., 2008; Stöhr, 2002; Tokars et al., 2018). The reason that best explains that the influenza virus can infect this proportion of the population every year is the fact that the influenza virus is able to evolve and, therefore, to avoid the immune response of individuals, i.e., immuno escape (Ballesteros, Vergu, & Cazelles, 2009; Park et al., 2009; Quiñones-Parra, Loh, Brown, Kedzierska, & Valkenburg, 2014; Yang, Lau, & Cowling, 2020).

2.4. Model parameters

This section is devoted to the presentation of the particular fixed values of the parameters of model (1) and also an explanation of the parameters that need to be calibrated. In addition, we show some details regarding how the initial conditions are computed.

2.4.1. Initial conditions

Some of the model parameters, for which we have information, were kept as fixed:

- The initial number of vaccinated and unvaccinated infected were fixed assuming that, at time $t = 0$, the epidemic begins with $I_u(0) = 1$ (the patient zero) and $I_v(0) = 0$ (the vaccination campaign had not yet started).
- The initial number of vaccinated and unvaccinated latents were set to $L_v(0) = \frac{\gamma}{\lambda}$, $I_v(0) = 0$ and $L_u(0) = \frac{\gamma}{\lambda}$, $I_u(0) = \frac{\gamma}{\lambda}$, to give continuity to the curves of the model. As an alternative, in (Chowell, 2017) it was assumed for simplicity that $E(0) = I(0)$ and then calibrated them.
- As initially there were no vaccinated people, the initial number of vaccinated recovered was $R_v(0) = 0$, so that the total recovered was $R(0) = R_u(0) + R_v(0) = R_u(0)$. This parameter, which is unknown, was identified in the calibration process, by analyzing multiple scenarios for the initial recovered condition, i.e., varying $R(0)$ from 0% to 95% of the total population N.
- The initial unvaccinated susceptible population is computed as

$$S_u(0) = N - I_u(0) - I_v(0) - L_u(0) - L_v(0) - R_u(0) - R_v(0), \tag{5}$$

while the initial number of vaccinated susceptibles is $S_v(0) = 0$.

2.4.2. Reporting fraction

In the calibration process, it also should be considered that, in the real world, there is a significant number of unreported cases (Jing, Huo, & Xiang, 2020; Magal & Webb, 2018). For instance, in (Reed et al., 2009) it was estimated that the ratio of

unreported to reported cases for the H1N1 influenza epidemic in the USA was 79 to 1. In another interesting work related to identifiability it was found that per each reported case there were approximately 37.7 unreported cases for the influenza season 2016–2017 in Puerto Rico in (Magal & Webb, 2018). In (Jing et al., 2020), it was found that several parameters that vary on time can have an impact on unreported cases. They found by a fitting process that only 5% of the influenza cases are reported.

We also know that only a proportion of infected vaccinated $k_v \in [0,1]$ and unvaccinated $k_u \in [0,1]$ are reported. Thus, in order to compare the model with the data, we establish that $I_{rv}(t) = k_v I_v(t)$ and that $I_{ru}(t) = k_u I_u(t)$.

It should be remarked that we are considering in our model that all the individuals who reach infected status (unvaccinated or vaccinated) have the same capacity to infect (a sufficient viral load) and have enough symptoms such that they can end up being reported, on average. Thanks to the vaccine attenuation factor a_v, the transition to this state of infection by vaccinated individuals is more difficult. Basically, the attenuation factor quantifies the difficulty of becoming infected. However, we are defining that infected vaccinated and unvaccinated individuals possess the same characteristics. Therefore, in this model, both infected groups - vaccinated and unvaccinated - enter the hospital in the same proportion, so $k_u = k_v = k$.

Given this consideration, we can define the following least-squares minimization problem

$$\min_{k\in[0,1]} \sum_{i=1}^{n} \left(kI_u(t_i) - I_{ru}^{t_i}\right)^2 + \sum_{i=1}^{n} \left(kI_v(t_i) - I_{rv}^{t_i}\right)^2. \tag{6}$$

The general solution for this optimization problem in terms of k is given by

$$\begin{aligned} \frac{d}{dk}\left[\sum_{i=1}^{n} \left(kI_u(t_i) - I_{ru}^{t_i}\right)^2 + \sum_{i=1}^{n} \left(kI_v(t_i) - I_{rv}^{t_i}\right)^2\right] &= 0, \\ \sum_{i=1}^{n} 2\left(kI_u(t_i) - I_{ru}^{t_i}\right)I_u(t_i) + \sum_{i=1}^{n} 2\left(kI_v(t_i) - I_{rv}^{t_i}\right)I_v(t_i) &= 0, \\ k\left(\sum_{i=1}^{n} I_u(t_i)^2 + \sum_{i=1}^{n} I_v(t_i)^2\right) - \sum_{i=1}^{n} I_{ru}^{t_i} I_u(t_i) - \sum_{i=1}^{n} I_{rv}^{t_i} I_v(t_i) &= 0, \\ k = \frac{\sum_{i=1}^{n} I_{ru}^{t_i} I_u(t_i) + \sum_{i=1}^{n} I_{rv}^{t_i} I_v(t_i)}{\sum_{i=1}^{n} I_u(t_i)^2 + \sum_{i=1}^{n} I_v(t_i)^2}. \end{aligned} \tag{7}$$

Note, that the value of k depends on the value of the transmission rate β and the vaccine attenuation factor a_v. Therefore, this parameter is also being implicitly calibrated. The least-squares minimization problem can be solved without formula (7) but it is more costly from a computational viewpoint. The parameter k does not affect the dynamics of the model, so the calibration process can be considered as depending on the parameters β and a_v. This parameter k is a scaling factor between the reported cases and the infected cases given by the model.

2.4.3. Calibrated parameters

For the calibration process two parameters, $\theta = (\beta, a_v)$, are calibrated while the others remain fixed. As we have mentioned above, the initial number of vaccinated and unvaccinated infecteds are set to $I_v(0) = 0$ and $I_u(0) = 1$. Using the fact that the infected population in one influenza season must remain between 5% and 15%, a narrower range of the infection rate $\beta \in \mathbb{R}_+$ can be given. To do so, the model was simulated

- for different values of β in a sufficiently large range: from 0 to 50, and 5000 values.
- for different values of initial recovered population $R(0) = R_u(0) + R_v(0)$. These values were chosen from 0% to 95% of the whole population N and separated by 5%, i.e., 20 values.
- for the most extreme cases for a_v, i.e., taking $a_v = 0$ (maximum vaccine efficacy), and $a_v = 1$ (zero vaccine efficacy). In the first case, only the unvaccinated will be infected, so the susceptible population is smaller, and therefore larger β values are needed in order to reach a total infected population of 5–15% at the end of the season. In the second case, the susceptible population is larger and smaller β values are required.

For all these simulations, the percentage of total infected people after the influenza season, or epidemic size, was computed as

$$\%I_{\text{total}} = \frac{R(t_n) - R(0)}{N},$$

where t_n is the last time instant registered at the end of the season. With this percentage, the smallest value of β reaching 5% and the largest value reaching 15% of total infected (using both a_v scenarios) were chosen as the calibration search interval

$\mathcal{I}_\beta = [\beta_{lo}, \beta_{up}]$ for the β parameter. Note that the 5–15% percentage of total infected people information is relevant for the calibration process since it allows us to obtain ranges for values of β. With this restriction added, the calibration process should not give values of β where the percentage of total infected people is more than 15% or less than 5% of the total population (Departamento de Seguridad Nacional, 2023; Russell et al., 2008; Stöhr, 2002; Tokars et al., 2018).

2.5. Calibration problem

The calibration process of the model was based on the classical estimation of the parameters by least-square fitting of the model solution to the data of the season 2016–2017 in the Valencian Community. The available data to calibrate the mathematical model consisted in two time series: unvaccinated $\{I_{ru}^{t_i}\}_{i=0}^{n}$ and vaccinated $\{I_{rv}^{t_i}\}_{i=0}^{n}$ reported infected cases. These series provide useful information in order to be able to calibrate the parameters (Magal & Webb, 2018; Raue et al., 2009). Regarding the calibration parameters, three model parameters were unknown at this point: β, a_v and $R(0) = R_u(0)$. The combination of these parameters affects the various aspects of the infected curve $I(t)$, changing the peak position, width, magnitude, etc. (Magal & Webb, 2018). However, all three parameters could not be calibrated at the same time, since the value of $R(0)$ modified the search range of another of the calibration parameters, β, so that the total infected people after the end of the season would be between 5 and 15% of the total population (see Section 2.4.3).

Thus, for the deterministic calibration process, given a parameters set $\theta = (\beta, a_v)$, the objective function have been defined as

$$\epsilon(\theta) = \epsilon_u(\theta) + \epsilon_v(\theta), \text{ where} \tag{8}$$

$$\epsilon_u(\theta) = \sum_{i=1}^{n} \left(kI_u(t_i;\theta) - I_{ru}^{t_i}\right)^2, \tag{9}$$

$$\epsilon_v(\theta) = \sum_{i=1}^{n} \left(kI_v(t_i;\theta) - I_{rv}^{t_i}\right)^2, \tag{10}$$

where k is given by Equation (7). As can be seen, this sum of squared errors (SSE) function tries to simultaneously minimize the error between the reported vaccinated and unvaccinated model solutions with their respective data series (Chowell, 2017). The minimization problem to be solved is

$$\theta^* = \underset{\theta \in \mathcal{I}_\beta \times [0,1]}{\arg\min} \{\epsilon(\theta)\}, \tag{11}$$

where $\mathcal{I}_\beta$ is the calibration search interval for the β parameter, which depends on the selected initial condition $R(0)$, as explained previously. This minimization problem is first solved for all values of $\%N$ as $R(0)$ (from 0.00 to 0.95, with 20 values). Subsequently, to obtain a more accurate value for $R(0)$, it is solved by choosing another 20 values of $R(0)$ between the upper and lower values surrounding the optimum $R(0)$ (smallest error) obtained in the stage of the calibration process.

The entire model simulation and calibration process is implemented in Matlab code. For the numerical solution of the model, the built-in function *ode45* (Runge-Kutta method of order 4 and 5) is used, while the minimization problem is solved with the *solve* built-in function, using the *GlobalSearch* input argument to guarantee a global minimum. It is important to remark that the calibration process computes simultaneously the values of the parameters β, a_v and k. However, the parameter k does not affect the dynamics of the mathematical model (1), but affects the global error $\varepsilon(\theta)$. On the other hand, the parameters β and a_v affect both the global error and the dynamics.

2.6. Error analysis

After obtaining the best $\%N$ as $R(0)$ initial condition, an analysis of the error function $\varepsilon(\theta)$ and its components $\varepsilon_u(\theta)$ and $\varepsilon_v(\theta)$, is performed. The objective of this error analysis is to test whether the observable data can be generated with a single $\varepsilon(\theta^*)$ (identifiable model parameters) or with multiple (unidentifiable model parameters). With all the information included in the model before the calibration and the available calibration dataset, and based on previous studies, it could be suggested that the unknown model parameters would be identifiable (Magal & Webb, 2018). To verify it, given the optimal initial recovered condition $R(0)^*$ found in the calibration, the error function was evaluated at multiple θ points, in order to observe the location of the minimum point $\theta^* = (\beta^*, a_v^*)$ and its neighborhood, and to assess whether the model parameters are identifiable.

3. Results and discussion

In this section we present the main results of the calibration process, and we also provide a discussion of the calibration results, specially about the vaccine efficacy estimation.

3.1. Search interval results

The graphical results of the β parameter search interval for all the calibration processes for different values for $R(0)$ are shown in Figs. 3 and 4. The specific numerical values for the range of the parameter search interval of β is given by $\mathcal{I}_\beta$ and it is shown in Table 3. As it can be expected, the range of the infection rate β is relatively small due to the high sensitivity of the model to this rate. Figs. 3 and 4 show the parameter search intervals $\mathcal{I}_\beta$ for a large and a refined range of $R(0)$, respectively. In all three panels of Figs. 3 and 4, it can be seen that the larger the initial recovered population $R(0)$ (i.e. smaller $S(0)$), the larger the infection rate should be in order to reach the 5–15% range of total infected in the whole season. In addition, it can be observed in the top panels that the smaller the vaccine attenuation factor a_v the larger the infection rate should be. In other words, when the efficacy of the vaccine $(1 - a_v)$ is high then the infection rate of the influenza should be higher too in order to achieve the 5–15% range. It is important to remark that with these different calibration search ranges $\mathcal{I}_\beta$ we are adding important information to the calibration process which helps to address identifiability aspects related to the calibrated parameters.

3.2. Calibration results

The numerical results of the least-squares minimization problem for a variety of initial conditions $R(0)$ are shown in Table 3. The top table shows the results with $\%N$ as $R(0)$ between 0 and 1, while the bottom one shows the same refined results, with $\%N$ as $R(0)$ between 0.70 and 0.80. In this way, the minimum can be detected more accurately. It can be observed that the lower the percentage of the initial population with previously acquired immunity, the higher the vaccine attenuation factor. This is because the initial susceptible population is much larger in these cases, and therefore it is easier for the virus to spread through the population (note that susceptibles regulate the infection strength in the $S(t)I(t)$ term of the model) (Hethcote, 2000). Thus, the vaccine attenuation factor a_v and infection rate β take lower values in order that the final epidemic size in an influenza season does not exceed the 15% of the total population (Departamento de Seguridad Nacional, 2023; Russell et al., 2008; Stöhr, 2002; Tokars et al., 2018). As a detail, it is observed that this relationship is not fulfilled in the range 0–20% of N as $R(0)$. This is because, for those β search ranges, the curve is highly distorted, since the peak of the infected season is

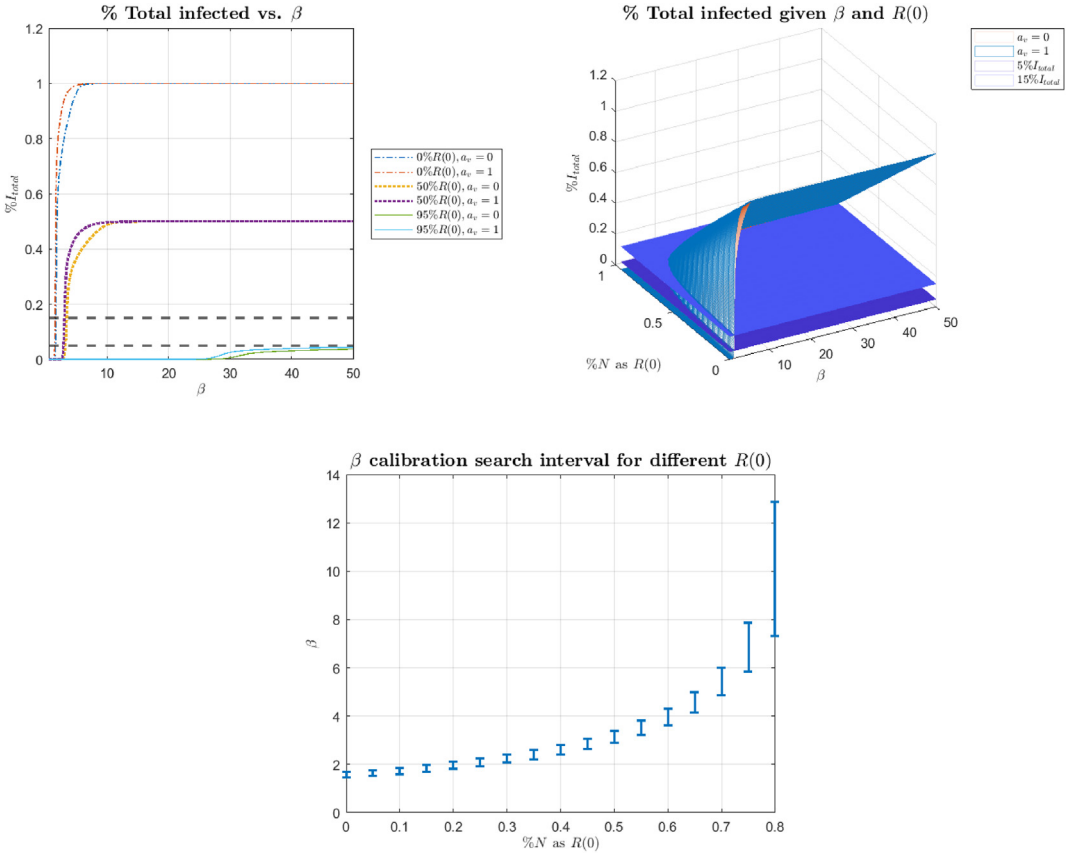

Fig. 3. β calibration search ranges $\mathcal{I}_\beta = [\beta_{lo}, \beta_{up}]$ for different $R(0)$ initial conditions.

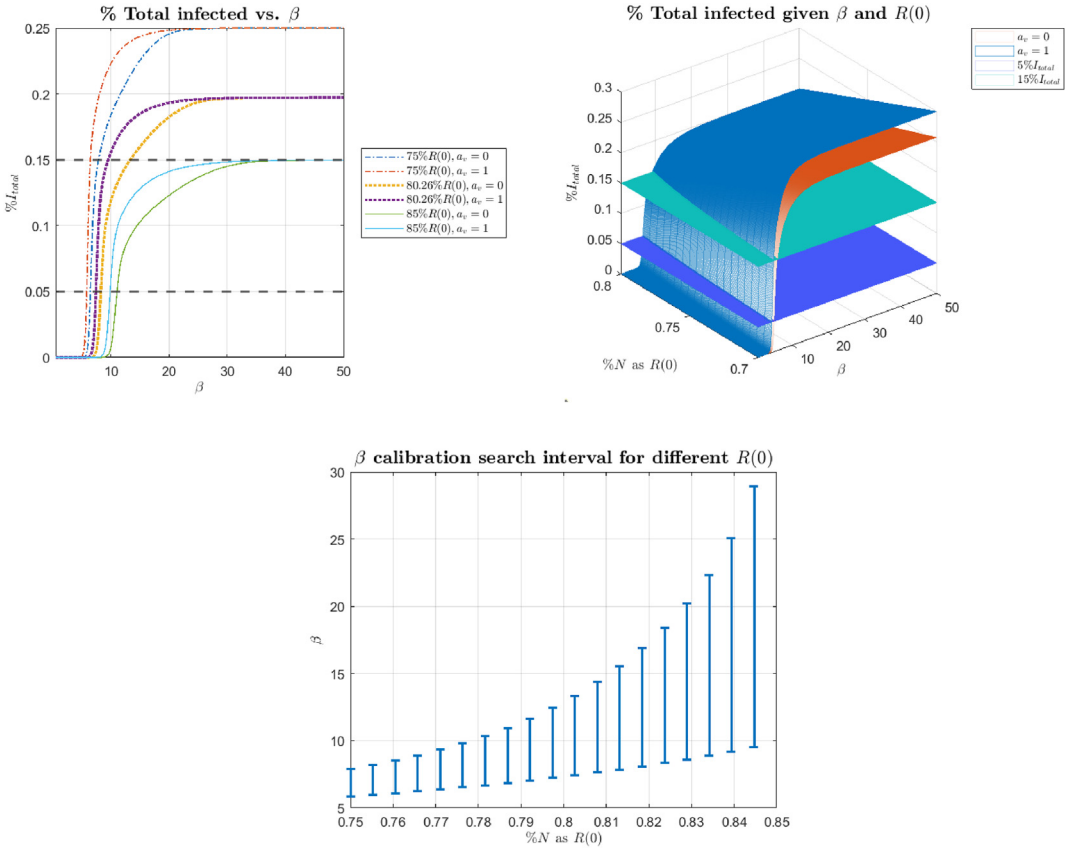

Fig. 4. β refined calibration search ranges $\mathcal{I}_\beta = [\beta_{lo}, \beta_{up}]$ for different $R(0)$ initial conditions.

outside the calibration time interval. Therefore, the algorithm chooses to try to decrease the magnitude of the curve as much as possible, reducing β and a_v as much as possible.

Fig. 5 shows the variation of the error for values of $R(0)$ varying in the range of 0–95% of N as $R(0)$ (left-hand side), and for a refined variation of values of $R(0)$ around the optimal region, i.e. 75-85% of N as $R(0)$ (right-hand side). The refined case shows more clearly the evolution of the error $\varepsilon(\theta)$ and the minimum error.

After calibration process we obtained the following optimal solution:

$$\theta^* = (\beta^*, a_v^*) = (9.1357, 0.2331),\ k^* = 0.0702,\ R(0)^* = 0.7711N,$$
$$\epsilon(\theta) = 4.7992 \times 10^6. \tag{12}$$

Of particular importance is the optimal value of k, which indicates that per each reported influenza case in the Valencian Community there are $1/0.0702 = 14.24$ unreported or undetected influenza cases. Notice that this number includes asymptomatic cases which can transmit the influenza virus. This result agrees with previous works where it has been estimated that per each reported case there are 79 unreported cases, with a 90% probability range of 47–148 (Reed et al., 2009). It has been mentioned that the reported cases for seasonal influenza are a small fraction of the total number of cases (Jing et al., 2020; Magal & Webb, 2018). For instance, in (Magal & Webb, 2018) it was found that per each reported case there were approximately 37.7 unreported cases for the influenza season 2016–2017 in Puerto Rico. In (Jing et al., 2020), it was found that several parameters that vary on time can have an impact on unreported cases. In our study, we have used time-invariant parameters since the study is for very short dynamics. However, using a non-autonomous model it has been found by a fitting process that only 5% of the influenza cases are reported (Jing et al., 2020).

Another important aspect related to the calibration process is that we have explored a variety of scenarios regarding the potential values of $R(0)$. Notice that this number represents all the individuals that have some previously acquired immunity before the seasonal influenza. The calibration process provides an optimal value for $R(0) = 0.7711\ N$, i.e. a huge mass of the population did not take part in the epidemic. This result suggest that the initial population has some form of acquired immunity before the start of the influenza season is approximately 77%. This value seems plausible due to cross-immunity from previous influenza strains and previous vaccinations (Karamitsou, 2021; Tricco et al., 2013). Other works have used a variety

Table 3
Calibration for different values of $R(0)$. On the top, the first calibration process, and on the bottom, the refined calibration. The optimal triplets for both calibrations are remarked in bold.

%N as $R(0)$	Range $\mathcal{I}_\beta$	Best (β, a_v, k)	$\varepsilon(\theta)$
0.0000	[1.4407, 1.6684]	(1.6684, 1.0000, 0.0028)	2.5978×10^8
0.0500	[1.5199, 1.7576]	(1.7576, 1.0000, 0.0033)	2.5841×10^8
0.1000	[1.5991, 1.8566]	(1.8566, 1.0000, 0.0036)	2.5796×10^8
0.1500	[1.6981, 1.9655]	(1.9655, 1.0000, 0.0036)	2.5864×10^8
0.2000	[1.8071, 2.0942]	(2.0942, 1.0000, 0.0047)	2.5538×10^8
0.2500	[1.9259, 2.2328]	(2.2328, 1.0000, 0.0041)	2.5901×10^8
0.3000	[2.0645, 2.4012]	(2.4012, 1.0000, 0.0056)	2.5458×10^8
0.3500	[2.2229, 2.5893]	(2.5893, 1.0000, 0.0066)	2.5209×10^8
0.4000	[2.4111, 2.8072]	(2.8072, 1.0000, 0.0069)	2.5342×10^8
0.4500	[2.6289, 3.0745]	(3.0745, 1.0000, 0.0077)	2.5313×10^8
0.5000	[2.8864, 3.4013]	(3.4013, 1.0000, 0.0103)	2.4658×10^8
0.5500	[3.2131, 3.7974]	(3.7974, 1.0000, 0.0128)	2.4158×10^8
0.6000	[3.6191, 4.3024]	(4.3024, 1.0000, 0.0161)	2.3505×10^8
0.6500	[4.1439, 4.9955]	(4.9955, 1.0000, 0.0231)	2.1478×10^8
0.7000	[4.8470, 5.9956]	(5.9956, 1.0000, 0.0359)	1.6715×10^8
0.7500	[5.8273, 7.8770]	(7.8770, 1.0000, 0.0594)	1.2315×10^7
0.8000	**[7.3225, 12.8577]**	**(10.3839, 0.2434, 0.0811)**	$\mathbf{4.8511 \times 10^6}$
0.8500	[9.8574, ∞]	(13.6264, 0.2769, 0.1099)	5.0306×10^6
0.9000	[15.2639, ∞]	(19.9591, 0.3428, 0.1685)	5.4351×10^6
0.9500	[0.5000, ∞]	(38.2259, 0.4879, 0.3495)	6.5672×10^6
%N as $R(0)$	Range $\mathcal{I}_\beta$	Best (β, a_v, k)	$\varepsilon(\theta)$
0.7500	[5.8273, 7.8770]	(7.8770, 1.0000, 0.0594)	1.2737×10^7
0.7553	[5.9560, 8.1839]	(8.1839, 0.9434, 0.0603)	7.6984×10^6
0.7605	[6.0847, 8.5305]	(8.5305, 0.6131, 0.0635)	6.0380×10^6
0.7658	[6.2332, 8.9068]	(8.9068, 0.2849, 0.0679)	4.8358×10^6
0.7711	**[6.3719, 9.3425]**	**(9.1357, 0.2331, 0.0702)**	$\mathbf{4.7992 \times 10^6}$
0.7763	[6.5303, 9.8178]	(9.3382, 0.2359, 0.0720)	4.8069×10^6
0.7816	[6.6887, 10.3525]	(9.5511, 0.2386, 0.0738)	4.8152×10^6
0.7868	[6.8571, 10.9565]	(9.7738, 0.2414, 0.0757)	4.8245×10^6
0.7921	[7.0353, 11.6397]	(10.0077, 0.2439, 0.0777)	4.8346×10^6
0.7974	[7.2234, 12.4220]	(10.2556, 0.2430, 0.0799)	4.8452×10^6
0.8026	[7.4215, 13.3330]	(10.5142, 0.2452, 0.0822)	4.8573×10^6
0.8079	[7.6294, 14.3628]	(10.7848, 0.2513, 0.0845)	4.8712×10^6
0.8132	[7.8473, 15.5411]	(11.0733, 0.2516, 0.0871)	4.8848×10^6
0.8184	[8.0849, 16.8779]	(11.3719, 0.2629, 0.0896)	4.9018×10^6
0.8237	[8.3325, 18.4127]	(11.6966, 0.2578, 0.0926)	4.9167×10^6
0.8289	[8.5998, 20.1950]	(12.0354, 0.2635, 0.0956)	4.9361×10^6
0.8342	[8.8870, 22.3438]	(12.3962, 0.2668, 0.0988)	4.9562×10^6
0.8395	[9.1840, 25.0668]	(12.7786, 0.2724, 0.1022)	4.9786×10^6
0.8447	[9.5108, 28.9088]	(13.1828, 0.2822, 0.1058)	5.0028×10^6
0.8500	[9.8574, ∞]	(13.6264, 0.2769, 0.1099)	5.0306×10^6

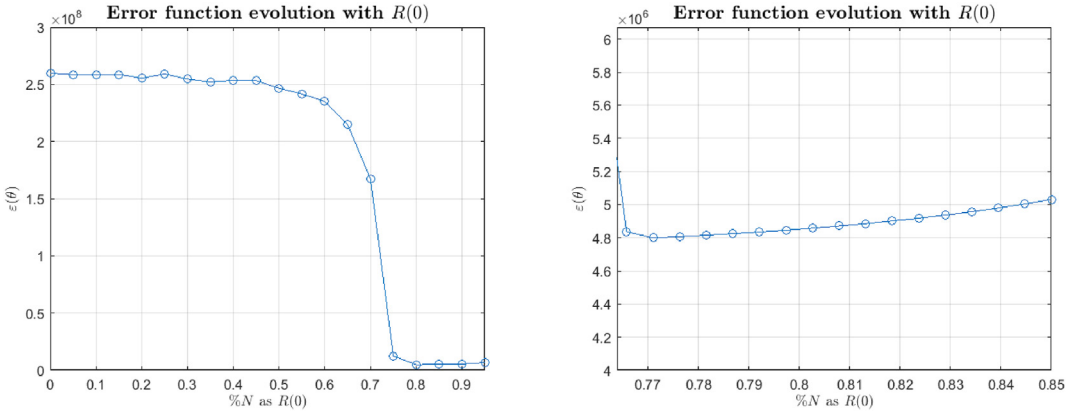

Fig. 5. Error function for different values of $R(0)$. On the left-hand side, the first calibration, and on the right-hand side, the refined calibration.

of values for the initial recovered population. For instance, in (Magal & Webb, 2018) the authors assumed that 1/3(33%) of the total population in Puerto Rico had acquired immunity against the influenza of 2016–2017 season and used this value in order to estimate the proportion of unreported cases, final epidemic size, basic reproduction number $\mathcal{R}_0$ and the infection rate of the virus. In (Ducrot, Magal, Nguyen, & Webb, 2020) the authors studied scenarios with a large variety of initial conditions for the susceptible population (and implicitly for the recovered one). In (Chowell, 2017), it was assumed that the whole population was susceptible in order to fit a SEIR model to seasonal influenza in the United States, France, and Australia. The variety of values of $R(0)$ implicitly determines a variety of initial conditions for the susceptible population. This is important since it has been mentioned that oftentimes the initial values of susceptible populations are unknown (Ducrot et al., 2020; Magal & Webb, 2018).

Fig. 6 shows the dynamics of each state variable for a numerical simulation of the model (1) by using the optimal values of the calibrated parameters. Fig. 7 shows the best fit of model (1) to the reported vaccinated and unvaccinated infected real data of the influenza season 2016–2017 in the Valencian Community. It can be seen that the calibration of the model to the data is relatively good despite the irregularity or noise of the data at the beginning of the influenza season. It can be observed the classical upward and downward dynamics over the season. The calibration to the vaccinated data is not as good as the vaccinated one due to the structure of the functional form of the error given by Equation (8). This can be improved by using different weights in the error functional but this topic is out of the scope of this article (for interested readers see (Chowell, 2017)). Besides the visual examination of the calibration we computed the goodness of fit by using the R-squared metric. The R-squared of the global error is 0.9726, the R-squared of the error related to the unvaccinated is 0.9730 and the R-squared related to the vaccinated error is 0.8560. These results agree with the visual examination and provide further robustness to the calibration process.

3.3. Error analysis results

Fig. 8 shows the error functions $\varepsilon_v(\theta)$, $\varepsilon_u(\theta)$ and $\varepsilon(\theta) = \varepsilon_u(\theta) + \varepsilon_v(\theta)$ for the particular value $R(0) = 0.7711\ N$ and varying the calibrated parameters β and a_v. If we combine both errors we can see that a global minimum is obtained. Note that, since $\varepsilon_u(\theta)$

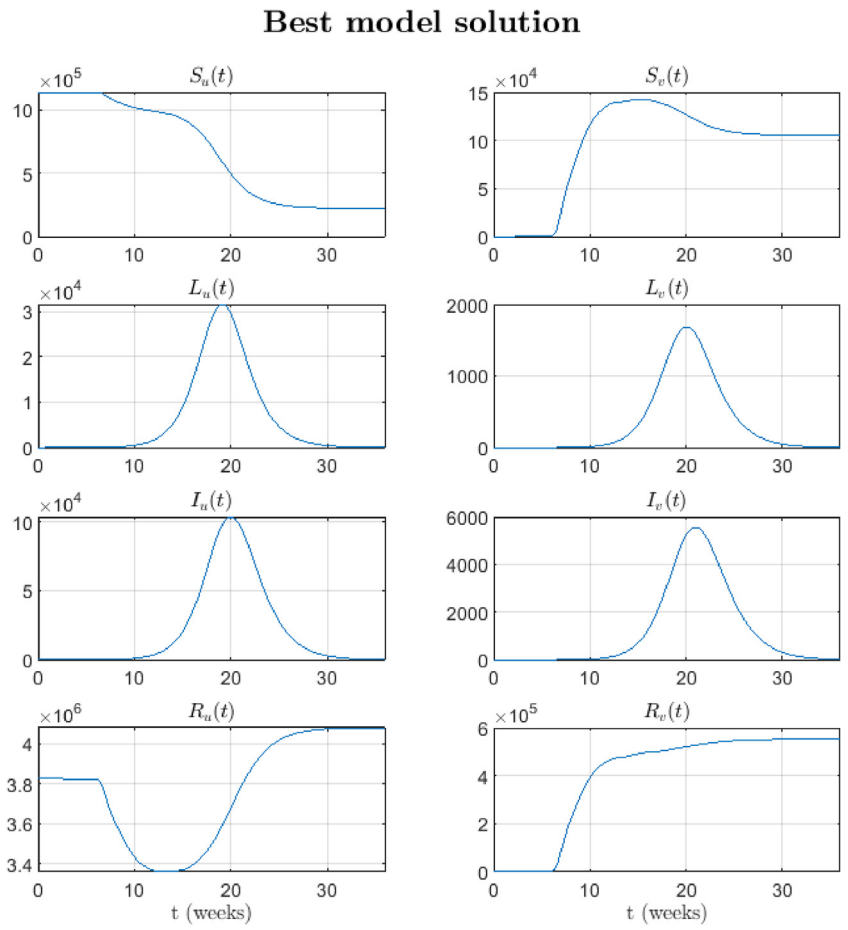

Fig. 6. Numerical simulation using the optimal solution θ^*. The dynamic profiles of all the state variables of model (1).

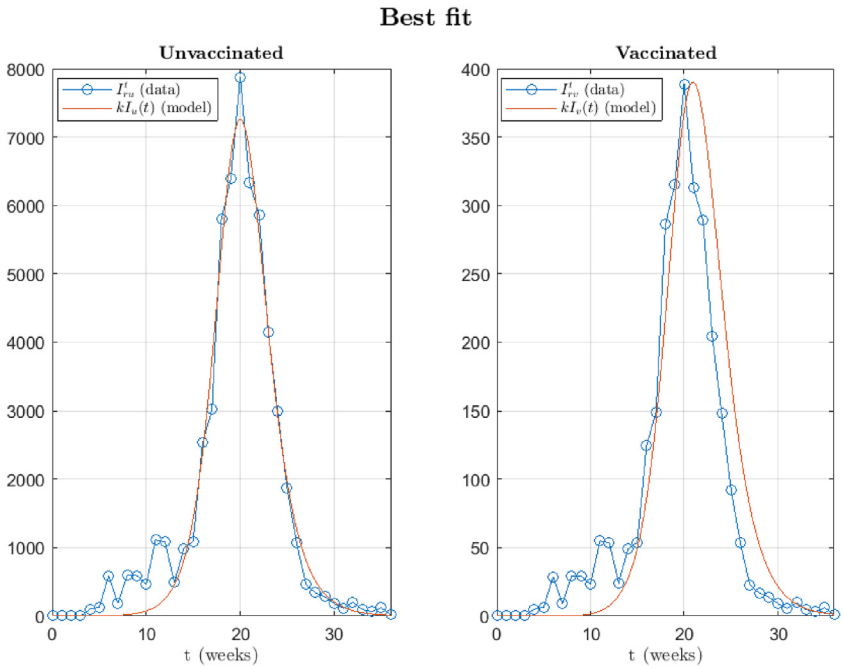

Fig. 7. Numerical simulation using the optimal solution θ^*. The profile of the infected populations of model (1).

is approximately two orders of magnitude larger than $\varepsilon_v(\theta)$, the total error function $\varepsilon(\theta)$ more closely resembles $\varepsilon_u(\theta)$ function. However, the separation allows us to appreciate the area of the minimum in $\varepsilon_v(\theta)$. This shows that, for this scenario, the calibration process obtained a global minimum and the model parameters are identifiable. This also can be inferred from the error analysis and the results presented in (Magal & Webb, 2018). As we have mentioned previously, this is due to the fact that we have all the initial conditions of the state variables and the calibration process takes advantage of using two time series. Furthermore, we have additional knowledge indicating that within a single influenza season, 5–15% of persons contract the influenza virus (Departamento de Seguridad Nacional, 2023; Russell et al., 2008; Stöhr, 2002; Tokars et al., 2018).

3.4. Vaccine efficacy results

In the section related to methods we have mentioned that there are a variety of methodologies to measure the vaccine efficacy. We explained that we use a vaccine efficacy interpretation that has been used by some authors even though there are other interpretations (Haber et al., 1991; Shim & Galvani, 2012). This interpretation states that the vaccine efficacy measures the variation in an individual risk of infection between those who have received the shot and those who have not. In the model (1) the model parameter a_v through the expression $1 - a_v$ is related to this interpretation. Thus, we have seen that based on the thorough calibration process the most likely value for the model embedded parameter a_v is approximately 0.23. This implies that we have obtained a vaccine efficacy around $(1 - 0.23) \times 100 = 77\%$ for the 2016–2017 influenza season. In other words, the vaccine reduces the likelihood to be infected by almost five times. This estimation is higher than one vaccine efficacy that is mentioned in (Diaz-Granados et al., 2012). However, is the range of vaccine efficacies from others previous studies (Demicheli, Jefferson, Ferroni, Rivetti, & Di Pietrantonj, 2018; Diaz-Granados et al., 2012). For instance, in (Flannery et al., 2018) it was estimated a vaccine efficacy for influenza as high as 73%. In addition, in (Benoit, Legrand, & Dewé, 2015) the authors found by simulations that is feasible that the influenza vaccine efficacy could be over 80% in most cases if the vaccine offers cross-protection. Therefore, we think that after the detailed calibration process and under the underlying assumptions of this study, the obtained vaccine efficacy value is feasible.

4. Conclusions

In this paper we designed and constructed a mathematical model to estimate the efficacy of the influenza vaccine in the Valencian Community in Spain. The model is a SEIR type epidemiological model that considers vaccinated and unvaccinated people. The model is based on a nonlinear system of ordinary differential equations where the nonlinearity is due to the effective contacts between susceptible and infected individuals. We used the reported cases of influenza of the 2016–2017 season in the Valencian Community in order to calibrate the model and obtain estimates for the efficacy of the influenza vaccine. The detailed calibration process takes into account that over one influenza season only a specific proportion of the

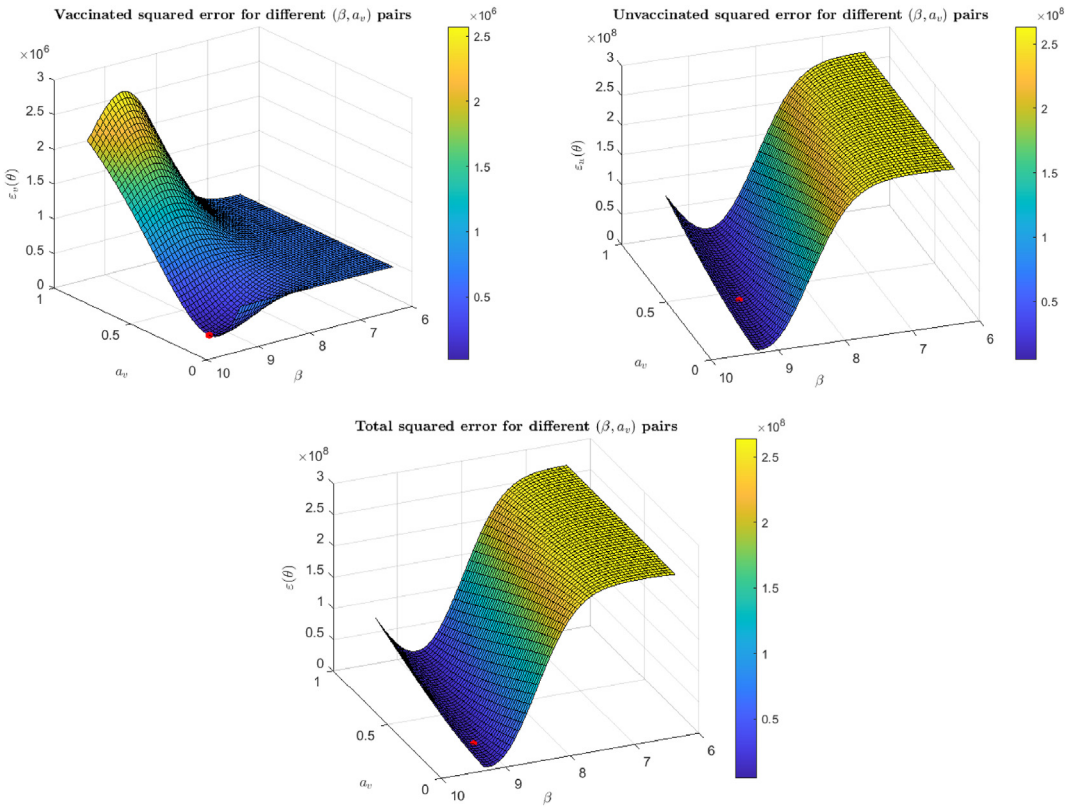

Fig. 8. Error functions $\varepsilon_v(\theta)$, $\varepsilon_u(\theta)$ and $\varepsilon(\theta)$ for the particular optimal value $R(0)^* = 0.7711$ N and varying the β and a_v parameters. The red point indicates the minimum.

population becomes infected with influenza. Based on the dynamics of influenza in the Valencian Community and the calibration results it is suggested that the influenza vaccine approximately reduces by one fifth the likelihood to become infected. We estimated that the influenza vaccine developed for the 2016–2017 influenza season had an efficacy around the 76.7%. This estimation depends on several factors that we have included in this research work. In this study we rely on relatively robust information regarding the number of people that gets infected in one season. This to the best of our knowledge has not been used in any previous study related to the estimation of the influenza vaccine efficacy. Identifying the reporting rate by only using the reported cases is very difficult. However, in this study, we used additional influenza epidemic information to estimate the reporting rate. For the estimation of the vaccine efficacy and calibration process we use two epidemic time series and take into account that over one influenza season a specific proportion of the population becomes infected with influenza. Another key aspect that we have used in this study is that we use a vaccine distribution that is based on real data specific to the elderly people in the Valencian Community. There are other factors that have not been included in the model due to the uncertainty, complexity and unfeasibility related to these factors. For instance, age has not been accounted explicitly in the model, even though some studies have mentioned that the age of individuals affect the efficacy of the vaccine. However, as it is common in mathematical epidemiology this approach implicitly aggregates or averages different factors over the whole population (Hethcote, 2000). Thus, the estimate of the vaccine efficacy provided in this study can be taken as an approximation to the exact value. The vaccine efficacy estimation obtained in this study partially agrees with some previous studies related to the influenza vaccine which in some way adds reliability to the study. Nevertheless, this estimate is subject to variability due to the uncertainty of the data and some values of the model parameters. In (Diaz-Granados et al., 2012) it was found from a review of thirty studies that the vaccine efficacy was 65% against any strain. This efficacy is lower that what it was obtained in this study. This could be due to the fact thta the influenza vaccine efficacy depends on many variables such as type of vaccine, age of vaccinees, level of matching to the circulating strains to the vaccine and the methodology to measure the efficacy (Diaz-Granados et al., 2012). Moreover, it could be possible that vaccinated people can have mild symptoms and therefore present a lower percentage of reporting. This would affect the estimation of the vaccine efficacy.

As in any mathematical model there are assumptions and limitations. Oftentimes, the limitations are associated with the assumptions made to design the model. In this study we have used real data regarding reported influenza cases in the Valencian Community, Spain. A key aspect of this study is that we used a vaccine distribution over time that is based on real

data specific to the elderly people in the Valencian Community. It might be possible that the vaccine distribution over time differs for other age groups. Thus, in our study it is assumed that most of the vaccinations occur before the peak of the influenza season. With regard to the unreported proportion in this study we assumed that it is time-invariant within a single influenza season. This in reality might be different, but including a time-dependent proportion can create identifiability issues due to the freedom of the functional form for the unreported proportion. With regard to the model, we know that any model is an approximation of the real world phenomenon. For instance, the age-structure often affects the dynamics. Also it has been found that the vaccine efficacy varies with age. The possibility that within a season some recovered people become susceptible has not been considered due to the short time span of one season, but this might affect the exact value of the vaccine efficacy. In addition, in the mathematical model, it is assumed that the vaccinated and unvaccinated populations have similar behaviors, but in reality, their behaviors could be different. This might affect the estimation of the vaccine efficacy. Another aspect that we should mention is that the outcomes of this study partially rely on previous information related to the final epidemic size for one influenza season (Departamento de Seguridad Nacional, 2023; Russell et al., 2008; Stöhr, 2002; Tokars et al., 2018). Thus, the results presented in this study should be taken with caution, if any of the assumptions of this study are not satisfied.

Finally, although the proposed mathematical approach considers the inherent uncertainty around some parameters of this complex problem, a deterministic (exact optimal value) calibration approach has been adopted to find the unknown parameters. As future lines, this approach could be extended to a random model, whose parameters are random variables, and a stochastic calibration for identification of the unknown parameters. To the best of our knowledge this is the first integrated mathematical approach that considers unreported cases, vaccine coverage, epidemic size for one influenza season and real data. For all these reasons, we think this study presents a plausible mathematical approach to study the influenza vaccine efficacy and gives further insight into this important public health topic.

Funding

The authors gratefully acknowledge financial support from the Spanish Health Instituto de Salud Carlos III (ISCIII) for the FIS PI21/01401 grant. Third author acknowledges grant María Zambrano (UPV, funding from the Spain Ministry of Universities funded by the European Union—Next Generation EU).

CRediT authorship contribution statement

Carlos Andreu-Vilarroig: Writing – review & editing, Writing – original draft, Visualization, Validation, Supervision, Software, Methodology, Investigation, Formal analysis, Data curation, Conceptualization. **Rafael J. Villanueva:** Writing – review & editing, Writing – original draft, Visualization, Validation, Supervision, Software, Resources, Project administration, Methodology, Investigation, Funding acquisition, Formal analysis, Data curation, Conceptualization. **Gilberto González-Parra:** Writing – review & editing, Writing – original draft, Visualization, Validation, Software, Methodology, Investigation, Formal analysis, Conceptualization.

Declaration of competing interest

All authors declare that they have no conflicts of interest.

Acknowledgments

The authors are grateful to the reviewers for their careful reading of this manuscript and their useful comments to improve the content of this paper.

References

Ballesteros, S., Vergu, E., & Cazelles, B. (2009). Influenza a gradual and epochal evolution: Insights from simple models. *PLoS One, 4*(10), Article e7426.
Basta, N. E., Halloran, M. E., Matrajt, L., & Longini, I. M., Jr. (2008). Estimating influenza vaccine efficacy from challenge and community-based study data. *American Journal of Epidemiology, 168*(12), 1343–1352.
Benoit, A., Legrand, C., & Dewé, W. (2015). Influenza vaccine efficacy trials: A simulation approach to understand failures from the past. *Pharmaceutical Statistics, 14*(4), 294–301.
Centers for Disease Control and Prevention (CDC). (2023). Influenza (flu). https://www.cdc.gov/flu/about/disease/spread.htm. (Accessed 27 October 2023).
Chadha, M., Hirve, S., Bancej, C., Barr, I., Baumeister, E., Caetano, B., et al. (2020). Human respiratory syncytial virus and influenza seasonality patterns—early findings from the who global respiratory syncytial virus surveillance. *Influenza and Other Respiratory Viruses, 14*(6), 638–646.
Chowell, G. (2017). Fitting dynamic models to epidemic outbreaks with quantified uncertainty: A primer for parameter uncertainty, identifiability, and forecasts. *Infectious Disease Modelling, 2*(3), 379–398.
Clar, C., Oseni, Z., Flowers, N., Keshtkar-Jahromi, M., & Rees, K. (2015). Influenza vaccines for preventing cardiovascular disease. *Cochrane Database of Systematic Reviews*.
Cole, D. (2020). *Parameter redundancy and identifiability*. CRC Press.
Demicheli, V., Jefferson, T., Ferroni, E., Rivetti, A., & Di Pietrantonj, C. (2018). Vaccines for preventing influenza in healthy adults. *Cochrane Database of Systematic Reviews, 2*(2).
Demongeot, J., Griette, Q., Magal, P., & Webb, G. (2022). Modeling vaccine efficacy for COVID-19 outbreak in New York city. *Biology, 11*(3), 345.

Departamento de Seguridad Nacional. (2023). Gripe: Evolución de la difusión geográfica en España. https://www.dsn.gob.es/es/actualidad/sala-prensa/gripe-estacional-y-su-actividad. (Accessed 3 November 2023).
Diaz-Granados, C. A., Denis, M., & Plotkin, S. (2012). Seasonal influenza vaccine efficacy and its determinants in children and non-elderly adults: A systematic review with meta-analyses of controlled trials. *Vaccine, 31*(1), 49–57.
Dombrádi, V., Joó, T., Palla, G., Pollner, P., & Belicza, É. (2021). Comparison of hesitancy between COVID-19 and seasonal influenza vaccinations within the general Hungarian population: A cross-sectional study. *BMC Public Health, 21*(1), 2317.
Ducrot, A., Magal, P., Nguyen, T., & Webb, G. (2020). Identifying the number of unreported cases in SIR epidemic models, mathematical medicine and biology: A journal of the IMA. *37*(2), 243–261.
European Centre for Disease Prevention and Control. (2018). Seasonal influenza vaccination and antiviral use in EU/EEA Member States. In *Overview of vaccine recommendations for 2017–2018 and vaccination coverage rates for 2015–2016 and 2016–2017 influenza seasons* [Online . (Accessed 22 January 2020).
Fadl, N., Al Awaidy, S. T., Elshabrawy, A., Makhlouf, M. S. A. H., Ibrahim, S. A., Abdel-Rahman, S., et al. (2023). Determinants of parental seasonal influenza vaccine hesitancy in the eastern mediterranean region: A cross-sectional study. *Frontiers in Public Health, 11*, Article 1132798.
Flannery, B., Chung, J. R., Belongia, E. A., McLean, H. Q., Gaglani, M., Murthy, K., et al. (2018). Interim estimates of 2017–18 seasonal influenza vaccine effectiveness—United States, February 2018. *American Journal of Transplantation, 18*(4), 1020–1025.
Gjini, E., & Gomes, M. G. M. (2016). Expanding vaccine efficacy estimation with dynamic models fitted to cross-sectional prevalence data post-licensure. *Epidemics, 14*, 71–82.
González-Parra, G., Villanueva, R.-J., Ruiz-Baragaño, J., & Moraño, J.-A. (2015). Modelling influenza A(H1N1) 2009 epidemics using a random network in a distributed computing environment. *Acta Tropica, 143*, 29–35.
Gumel, A. B., Iboi, E. A., Ngonghala, C. N., & Elbasha, E. H. (2021). A primer on using mathematics to understand COVID-19 dynamics: Modeling, analysis and simulations. *Infectious Disease Modelling, 6*, 148–168.
Gupta, V., Earl, D. J., & Deem, M. W. (2006). Quantifying influenza vaccine efficacy and antigenic distance. *Vaccine, 24*(18), 3881–3888.
Haber, M., Longini, I. M., JR., & Halloran, M. E. (1991). Measures of the effects of vaccination in a randomly mixing population. *International Journal of Epidemiology, 20*(1), 300–310.
Halloran, M. E., Struchiner, C. J., & Longini, I. M., Jr. (1997). Study designs for evaluating different efficacy and effectiveness aspects of vaccines. *American Journal of Epidemiology, 146*(10), 789–803.
Hethcote, H. W. (1994). A thousand and one epidemic models. In *Frontiers in mathematical biology* (pp. 504–515). Springer.
Hethcote, H. W. (2000). The mathematics of infectious diseases. *SIAM Review, 42*(4), 599–653.
Hethcote, H. W., & van den Driessche, P. (1991). Some epidemiological models with nonlinear incidence. *Journal of Mathematical Biology, 29*(3), 271–287.
Hirve, S., Newman, L. P., Paget, J., Azziz-Baumgartner, E., Fitzner, J., Bhat, N., et al. (2016). Influenza seasonality in the tropics and subtropics–when to vaccinate? *PLoS One, 11*(4), Article e0153003.
Hughes, M. M., Reed, C., Flannery, B., Garg, S., Singleton, J. A., Fry, A. M., et al. (2020). Projected population benefit of increased effectiveness and coverage of influenza vaccination on influenza burden in the United States. *Clinical Infectious Diseases, 70*(12), 2496–2502.
Instituto Nacional de Estadística (INE). (2023). *Indicadores demográficos básicos*. https://www.ine.es/. (Accessed 28 October 2023).
Jefferson, T., Rivetti, A., Harnden, A., Di Pietrantonj, C., & Demicheli, V. (2008). Vaccines for preventing influenza in healthy children. *Cochrane Database of Systematic Reviews*, (2).
Jing, S.-L., Huo, H.-F., & Xiang, H. (2020). Modeling the effects of meteorological factors and unreported cases on seasonal influenza outbreaks in Gansu province, China. *Bulletin of Mathematical Biology, 82*, 1–36.
Johansen, N. D., Modin, D., Skaarup, K. G., Nealon, J., Samson, S., Dufournet, M., et al. (2024). Effectiveness of high-dose vs. standard-dose quadrivalent influenza vaccine against recurrent hospitalisations and mortality in relation to influenza circulation: A post-hoc analysis of the danflu-1 randomised clinical trial. *Clinical Microbiology and Infection*.
Karamitsou, V. (2021). *A cross-scale model for the evolution of influenza within a single season*. University of Cambridge. Ph.D. thesis.
Kissling, E., & Rondy, M. (2017). I-MOVE/I-MOVE+ study team, early 2016/17 vaccine effectiveness estimates against influenza A(H3N2): I-MOVE multicentre case control studies at primary care and hospital levels in Europe. *Euro Surveillance, 22*(7).
Kreutz, C., Raue, A., & Timmer, J. (2012). Likelihood based observability analysis and confidence intervals for predictions of dynamic models. *BMC Systems Biology, 6*(1), 1–9.
Lopez, C. E., & Legge, K. L. (2020). Influenza A virus vaccination: Immunity, protection, and recent advances toward a universal vaccine. *Vaccines, 8*(3), 434.
Macdonald, P., & Lyth, J. (1918). Incubation period of influenza. *British Medical Journal, 2*(3018), 488.
Magal, P., & Webb, G. (2018). The parameter identification problem for SIR epidemic models: Identifying unreported cases. *Journal of Mathematical Biology, 77*, 1629–1648.
Mahmud, M. S., Kamrujjaman, M., Adan, M. M. I. Y., Hossain, M. A., Rahman, M. M., Islam, M. S., et al. (2022). Vaccine efficacy and SARS-CoV-2 control in California and US during the session 2020–2026: A modeling study. *Infectious Disease Modelling, 7*(1), 62–81.
Martínez-Rodríguez, D., Gonzalez-Parra, G., & Villanueva, R.-J. (2021). Analysis of key factors of a SARS-CoV-2 vaccination program: A mathematical modeling approach. *Epidemiologia, 2*(2), 140–161.
Martínez-Rodríguez, D., Navarro-Quiles, A., San-Julián-Garcés, R., & Villanueva, R.-J. (2020). A computational procedure to capture the data uncertainty in a model calibration: The case of the estimation of the effectiveness of the influenza vaccine. In *Lecture notes in mechanical engineering* (pp. 374–382). Springer International Publishing.
Mercer, G. N., Barry, S. I., & Kelly, H. (2011). Modelling the effect of seasonal influenza vaccination on the risk of pandemic influenza infection. *BMC Public Health, 11*(1), 1–10.
Morimoto, N., & Takeishi, K. (2018). Change in the efficacy of influenza vaccination after repeated inoculation under antigenic mismatch: A systematic review and meta-analysis. *Vaccine, 36*(7), 949–957.
Nishiura, H., & Chowell, G. (2009). *The effective reproduction number as a prelude to statistical estimation of time-dependent epidemic trends, Mathematical and statistical estimation approaches in epidemiology* (pp. 103–121).
Park, A. W., Daly, J. M., Lewis, N. S., Smith, D. J., Wood, J. L., & Grenfell, B. T. (2009). Quantifying the impact of immune escape on transmission dynamics of influenza. *Science, 326*(5953), 726–728.
Paules, C. I., Sullivan, S. G., Subbarao, K., & Fauci, A. S. (2018). Chasing seasonal influenza—the need for a universal influenza vaccine. *New England Journal of Medicine, 378*(1), 7–9.
Poetri, O., Bouma, A., Claassen, I., Koch, G., Soejoedono, R., Stegeman, A., et al. (2011). A single vaccination of commercial broilers does not reduce transmission of H5N1 highly pathogenic avian influenza. *Veterinary Research, 42*(1), 1–12.
Portero, A., Alguacil, A. M., Sanchis, A., Pastor, E., López, A., Miralles, M. T., et al. (2017). Prevención y vigilancia de la gripe en la Comunitat Valenciana. Temporada 2016-2017 (Prevention and surveillance of the influenza in the Community of Valencia. Season 2016-2017, Generalitat Valenciana. *Conselleria de Sanitat Universal i Salut Pública*.
Portero de la Cruz, S., & Cebrino, J. (2020). Trends, coverage and influencing determinants of influenza vaccination in the elderly: A population-based national survey in Spain (2006–2017). *Vaccines, 8*(2), 327.
Quach, T. H. T., Mallis, N. A., & Cordero, J. F. (2020). Influenza vaccine efficacy and effectiveness in pregnant women: Systematic review and meta-analysis. *Maternal and Child Health Journal, 24*, 229–240.
Quiñones-Parra, S., Loh, L., Brown, L. E., Kedzierska, K., & Valkenburg, S. A. (2014). Universal immunity to influenza must outwit immune evasion. *Frontiers in Microbiology, 5*, 285.

Ratti, M., Concina, D., Rinaldi, M., Salinelli, E., Di Brisco, A. M., Ferrante, D., et al. (2022). Vaccination strategies against seasonal influenza in long term care setting: Lessons from a mathematical modelling study. *Vaccines, 11*(1), 32.
Raue, A., Kreutz, C., Maiwald, T., Bachmann, J., Schilling, M., Klingmüller, U., et al. (2009). Structural and practical identifiability analysis of partially observed dynamical models by exploiting the profile likelihood. *Bioinformatics, 25*(15), 1923–1929.
Raue, A., Kreutz, C., Theis, F. J., & Timmer, J. (2013). Joining forces of Bayesian and frequentist methodology: A study for inference in the presence of non-identifiability. *Philosophical Transactions of the Royal Society A: Mathematical, Physical & Engineering Sciences, 371*(1984), Article 20110544.
Reed, C., Angulo, F. J., Swerdlow, D. L., Lipsitch, M., Meltzer, M. I., Jernigan, D., et al. (2009). Estimates of the prevalence of pandemic (H1N1) 2009, United States, april–july 2009. *Emerging Infectious Diseases, 15*(12), 2004.
Romagosa, A., Allerson, M., Gramer, M., Joo, H. S., Deen, J., Detmer, S., et al. (2011). Vaccination of influenza a virus decreases transmission rates in pigs. *Veterinary Research, 42*, 1–15.
Russell, C. A., Jones, T. C., Barr, I. G., Cox, N. J., Garten, R. J., Gregory, V., et al. (2008). Influenza vaccine strain selection and recent studies on the global migration of seasonal influenza viruses. *Vaccine, 26*, D31–D34.
Shim, E., & Galvani, A. P. (2012). Distinguishing vaccine efficacy and effectiveness. *Vaccine, 30*(47), 6700–6705.
Stöhr, K. (2002). Influenza—who cares. *The Lancet Infectious Diseases, 2*(9), 517.
Tamerius, J., Nelson, M. I., Zhou, S. Z., Viboud, C., Miller, M. A., & Alonso, W. J. (2011). Global influenza seasonality: Reconciling patterns across temperate and tropical regions. *Environmental Health Perspectives, 119*(4), 439–445.
Tentori, K., Passerini, A., Timberlake, B., & Pighin, S. (2021). The misunderstanding of vaccine efficacy. *Social Science & Medicine, 289*, Article 114273.
Tokars, J. I., Olsen, S. J., & Reed, C. (2018). Seasonal incidence of symptomatic influenza in the United States. *Clinical Infectious Diseases, 66*(10), 1511–1518.
Tricco, A. C., Chit, A., Soobiah, C., Hallett, D., Meier, G., Chen, M. H., et al. (2013). Comparing influenza vaccine efficacy against mismatched and matched strains: A systematic review and meta-analysis. *BMC Medicine, 11*, 1–19.
Valenciana, G. (2023). Sanitat inicia la campaña contra la gripe con el objetivo de aumentar la vacunación entre mayores de 60 años, profesionales sanitarios y los grupos de riesgo. https://comunica.gva.es/es/detalle?id=360079077&site=174859789. (Accessed 3 November 2023).
van der Goot, J. A., van Boven, M., Koch, G., & de Jong, M. C. (2007). Variable effect of vaccination against highly pathogenic avian influenza (H7N7) virus on disease and transmission in pheasants and teals. *Vaccine, 25*(49), 8318–8325.
Van Effelterre, T., Dos Santos, G., & Shinde, V. (2016). Twin peaks: A/H1N1 pandemic influenza virus infection and vaccination in Norway, 2009–2010. *PLoS One, 11*(3), Article e0151575.
Vila-Candel, R., Navarro-Illana, P., Navarro-Illana, E., Castro-Sánchez, E., Duke, K., Soriano-Vidal, F. J., et al. (2016). Determinants of seasonal influenza vaccination in pregnant women in Valencia, Spain. *BMC Public Health, 16*, 1–7.
Warren-Gash, C., Smeeth, L., & Hayward, A. C. (2009). Influenza as a trigger for acute myocardial infarction or death from cardiovascular disease: A systematic review. *The Lancet Infectious Diseases, 9*(10), 601–610.
Weinberg, G. A., & Szilagyi, P. G. (2010). Vaccine epidemiology: Efficacy, effectiveness, and the translational research roadmap. *The Journal of Infectious Diseases, 201*(11), 1607–1610.
World Health Organization (WHO). (2023). Influenza (seasonal). https://www.who.int/en/news-room/fact-sheets/detail/influenza-(seasonal. (Accessed 11 November 2023).
Yang, W., Lau, E. H., & Cowling, B. J. (2020). Dynamic interactions of influenza viruses in Hong Kong during 1998-2018. *PLoS Computational Biology, 16*(6), Article e1007989.
Yin, L., Lu, Y., Du, C., & Shi, L. (2022). Effect of vaccine efficacy on disease transmission with age-structured. *Chaos, Solitons & Fractals, 156*, Article 111812.
Young, B. E., & Chen, M. (2020). Influenza in temperate and tropical Asia: A review of epidemiology and vaccinology. *Human Vaccines & Immunotherapeutics, 16*(7), 1659–1667.
Yuan, H., Kramer, S. C., Lau, E. H., Cowling, B. J., & Yang, W. (2021). Modeling influenza seasonality in the tropics and subtropics. *PLoS Computational Biology, 17*(6), Article e1009050.
Zhang, X.-S., Pebody, R., De Angelis, D., White, P. J., Charlett, A., & McCauley, J. W. (2014). The possible impact of vaccination for seasonal influenza on emergence of pandemic influenza via reassortment. *PLoS One, 9*(12), Article e114637.